Ionic Selectivity of I_h Channels of Rod Photoreceptors in Tiger Salamanders

LONNIE P. WOLLMUTH and BERTIL HILLE

From the Department of Physiology and Biophysics, University of Washington School of Medicine, Seattle, Washington 98195

ABSTRACT Ionic selectivity of I_h channels of tiger salamander rod photoreceptors was investigated using whole-cell voltage clamp. Measured reversal potentials and the Goldman-Hodgkin-Katz voltage equation were used to calculate permeability ratios with 20 mM K^+ as a reference. In the absence of external K^+, I_h is small and hard to discern. Hence, we defined I_h as the current blocked by 2 mM external Cs^+. Some small amines permeate I_h channels, with the following permeability ratios (P_X/P_K):NH_4^+, 0.17; methylammonium, 0.06; and hydrazine, 0.04. Other amines are tially impermeant: dimethylammonium (<0.02), ethylammonium (<0.01), and tetramethylammonium (<0.01). When K^+ is the only external permeant ion and its concentration is varied, the reversal potential of I_h follows the Nernst potential for a K^+ electrode. I_h channels are also permeable to other alkali metal cations (P_X/P_K): Tl^+, >1.55; K^+, 1; Rb^+, >0.55; Na^+, 0.33; Li^+, 0.02. Except for Na^+, the relative slope conductance had a similar sequence (G_X/G_K): Tl^+, 1.07; K^+, 1; Rb^+, 0.37; NH_4^+, 0.07; Na^+, 0.02. Based on permeabilities to organic cations, the narrowest part of the pore has a diameter between 4.0 and 4.6 Å. Some permeant cations have large effects on the gating kinetics of I_h channels; however, permeant cations appear to have little effect on the steady-state activation curve of I_h channels. Lowering K^+ or replacing K^+ with Na^+ reduces the maximal conductance of I_h but does not shift or change the steepness of its voltage dependence. With ammonium or methylammonium replacing K^+ a similar pattern is seen, except that there is a small positive shift of ~10 mV in the voltage dependence.

INTRODUCTION

I_h (also called I_f or I_Q) is a steeply voltage-gated current activated by membrane hyperpolarization (Bader, Macleish, and Schwartz, 1979; Attwell and Wilson, 1980; Yanagihara and Irisawa, 1980; DiFrancesco, 1981*a*; Attwell, Werblin, and Wilson, 1982; Bader, Bertrand, and Schwartz, 1982; Spain, Schwindt, and Crill, 1987; Barnes and Hille, 1989). Channels underlying I_h are permeable to both K^+ and Na^+ and appear quite selective for these ions (DiFrancesco, 1981*b*; Mayer and Westbrook, 1983; Bader and Bertrand, 1984; Edman and Grampp, 1989). This selectivity profile differs from those for other channel types. K and Na channels are highly selective for

Address reprint requests to Dr. Bertil Hille, Department of Physiology and Biophysics, SJ-40, University of Washington School of Medicine, Seattle, WA 98195.

J. GEN. PHYSIOL. © The Rockefeller University Press · 0022-1295/92/11/0749/17 $2.00
Volume 100 November 1992 749–765

K^+ or Na^+, respectively, whereas nonselective cation channels like the nicotinic acetylcholine receptor (nAChR) channel are highly permeable to all alkali metals, as well as to many other inorganic and organic cations (Adams, Dwyer, and Hille, 1980; Dwyer, Adams, and Hille, 1980). A detailed study looking at a large number of potentially permeant ions in I_h channels is needed if we are to analyze the permeation mechanism. Here we quantify ion selectivity in I_h channels using changes in reversal potentials under biionic conditions.

Some of this work has appeared in abstract form (Wollmuth and Hille, 1991, 1992).

MATERIALS AND METHODS

Isolation of Rod Photoreceptors

Rod photoreceptors were isolated mechanically from the retina of aquatic tiger salamanders (*Ambystoma tigrinum;* Kons Scientific Co., Inc., Germantown, WI). Salamanders were maintained at room temperature with ambient illumination for at least 24 h before preparation. An animal was decapitated, the head was hemisected, and the eyeballs were removed. The retina was isolated from the eyeball and a cell suspension was made by triturating the retina in Ringer's solution using a cut-off, fire-polished Pasteur pipette. Recordings were made from solitary rods under constant bright light from the microscope illuminator.

Solutions

Internal. The pipette solution consisted of (mM): 100 KCl, 3.5 $MgCl_2$, 10 HEPES, 1 EGTA, and 1.5 K_2ATP, pH adjusted to 7.4 with KOH. The total K^+ concentration was 108 mM. EGTA and ATP were obtained from Sigma Chemical Co. (St. Louis, MO) and HEPES was from Calbiochem Corp. (La Jolla, CA).

External. To measure permeability ratios, we used a 20 mM KCl solution as a reference (mM): 20 KCl, 90 tetraethylammonium Cl (TEACl), 8 or 16 glucose, and 5 histidine, pH adjusted to 7.4 with HCl. These solutions minimize other currents that may contaminate I_h, including a delayed rectifier K^+ current (blocked by TEA) and Ca^{2+}-activated K^+ and Cl^- currents (0 external Ca^{2+}, EGTA in pipette, and TEA outside) (Bader et al., 1982). TEA also removes much but not all of a K^+ current called I_{Kx} (Beech and Barnes, 1989). In a few experiments, 2 mM $BaCl_2$ and 0.1 mM $CdCl_2$ were added. In test solutions, the 20 mM KCl was replaced by an equivalent amount of various test cations as the chloride salt. For hydrazine, in both the reference and test solutions, the buffer was 10 mM 2-[*N*-morpholino] ethanesulfonic acid (MES) instead of 5 mM histidine and the pH was adjusted to 5.75 with TMAOH. In solutions used to measure permeability to Tl^+, the anion was NO_3^- and 20 mM $TlNO_3$ replaced 20 mM KNO_3 in the test solution. At times we used a control solution that consisted of (mM): 20 KCl, 30 *N*-methyl-D-glucamine (NMDG), 60 TEACl, 16 glucose, and 5 histidine, pH adjusted to 7.4 with HCl. The NMDG was replaced by an equivalent amount of a test cation. In testing different K^+ concentrations, we used this control solution and kept the sum of the NMDG and K^+ concentrations constant at 50 mM.

Whole-Cell Recording

The whole-cell version of the patch clamp technique (Hamill, Marty, Neher, Sakmann, and Sigworth, 1981) was used to voltage clamp and dialyze cells at room temperature (21–25°C). Electrodes were pulled from glass hematocrit tubes (VWR Scientific Corp., Seattle, WA) and had resistances of 2–5 MΩ when filled with the pipette solution and measured in the 20-mM K^+

reference solution. The pipette was sealed to the inner segment of the photoreceptor, the patch was broken by suction, and whole-cell membrane current was measured using an Axopatch 1-C patch clamp (Axon Instruments, Inc., Foster City, CA). Currents were recorded with partial pipette and membrane capacitance compensation, low-pass filtered at 200 Hz, digitized at 1 kHz, and stored and analyzed on an IBM-compatible computer using the BASIC-FASTLAB software and hardware package (INDEC systems, Inc., Capitola, CA). Boltzmann and Hill equations were fitted using nonlinear least squares. Results are reported as mean ± SEM.

The recording chamber consisted of three connected wells cut out from a layer of Sylgard at the bottom of a Petri dish. Cell suspensions were pipetted into the center and largest well (100–200 μl). The two end chambers were the inflow and outflow for superfusion. Tests with dyes indicated that bath solutions were mostly exchanged within 30 s. For all experiments, solution flow was continuous.

Liquid-junction potentials were measured using a Beckman ceramic-junction, saturated KCl electrode and were corrected during data analysis. The junction potential between the 20 mM K^+ reference solution and the pipette solution was −3 mV (pipette negative). Superfusion of some test cation solutions generated junction potentials between the ground electrode and bath of 1 mV (NaCl, amines), 2 mV (LiCl), or −1 mV (KNO_3, $TlNO_3$) (ground electrode 0 mV).

Evaluation of I_h steady-state activation curves. We used tail current amplitudes measured 10 ms after a test step to construct I_h activation curves. Tail amplitudes were converted to conductance by dividing the current by the driving force ($E - E_r$), where E is the tail potential and E_r the reversal potential for I_h. Conductance–voltage plots were fitted with the Boltzmann equation:

$$g(E) = g_{max}/[1 + \exp[(E - E_{1/2})/S]]$$

where g is conductance, g_{max} is the maximal conductance, $E_{1/2}$ is the voltage for half-maximal activation, and S is the slope factor. The slope factor was converted into equivalent gating charge (Q) by dividing RT/F by the measured slope factor. R, T, and F have their normal thermodynamic meanings and the quantity RT/F was 25.5 mV (22°C). Q is an index of the number of charges needed to move all the way across the membrane for channel gating to occur (Hodgkin and Huxley, 1952).

Ionic selectivity. Permeability ratios were determined with the Goldman-Hodgkin-Katz (GHK) voltage equation (Goldman, 1943; Hodgkin and Katz, 1949). If one assumes that K^+ and Na^+ are the only permeant ions, it has the form:

$$E_r = (RT/F) \ln [(P_K[K]_o + P_{Na}[Na]_o)/(P_K[K]_i + P_{Na}[Na]_i)]$$

where E_r is the zero current or reversal potential.

Ionic selectivity of I_h channels was determined by measuring the change of reversal potential for I_h on replacing the 20 mM K^+ reference solution, which contains no Na^+ or other permeant ion, with an identical solution except with the K^+ replaced by a test cation, X^+. The permeability ratios, P_X/P_K, were calculated according to the relation:

$$E_{r,X} - E_{r,K} = \Delta E_r = (RT/F) \ln [(P_X[X]_o/P_K[K]_o)]$$

This equation is valid only if the internal concentrations of permeant ions remain constant. To avoid large ionic fluxes, we used short conditioning voltage steps (0.2 s).

In the voltage range negative to −33 mV, rod photoreceptor membranes exhibit two major voltage- and time-dependent conductances, those of I_h and I_{Kx} channels (Beech and Barnes, 1989; Wollmuth, L. P., unpublished observations). The I_{Kx} channels are open at −33 mV and close slowly during hyperpolarization, and I_h channels are shut at −33 mV and open slowly during hyperpolarization. Despite the presence of TEA in our solutions, a residual component of I_{Kx} contaminates the first 50 ms of a hyperpolarizing step, particularly when the bathing

solution contains ions that are quite permeant in K^+ channels (K^+, Tl^+, Rb^+, NH_4^+). Since 2 mM Cs^+ blocks much of I_h without blocking I_{Kx}, most experiments used a Cs^+ subtraction procedure described in Results to remove the contaminating I_{Kx}.

To measure reversal potentials, we used a standard protocol. After break-in to the whole-cell configuration and waiting 3–4 min for intracellular dialysis, we recorded currents in the 20 mM K^+ reference solution and then in the same solution but with 2 mM CsCl added. Subsequently, we perfused the test solution a minimum of 3 min (~20–40 vol of solution through the chamber). We then recorded currents in the test solution and again in the same solution but with 2 mM CsCl added. In most instances we then retested the 20 K reference solution. In comparison to the pre-20 K, the post-20 K reversal potential never changed by more than 3 mV. When both pre- and post-20 K reversal potentials were measured, they were averaged in calculating changes in reversal potential.

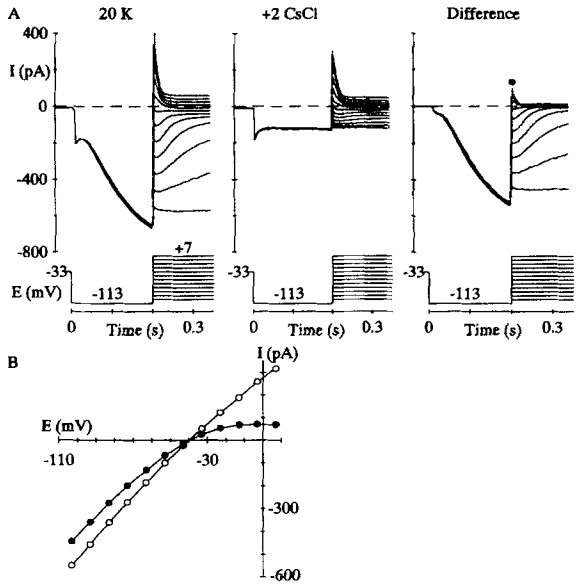

FIGURE 1. Reversal of I_h. (*A*) Whole-cell currents from a rod bathed in 20 mM KCl, 90 mM TEACl with 0 (*left*) or 2 mM (*center*) added CsCl. The difference between currents in 0 and 2 mM Cs^+ is shown on the right. Holding potential was −33 mV, indicated at the beginning of the voltage trace, and test steps were in 10-mV increments with 4-s intervals between steps. (*B*) Instantaneous current amplitude (measured 10 ms after the start of the test step) plotted against test step potential (*I-E* relation). Points derived from the Cs^+-difference current (*filled circles*) or by linear leak subtraction of the 0 Cs^+ record (*open circles*). Leak subtraction was performed by scaling a record, produced by stepping from −33 to −43 mV for 0.2 s and returning to −33 mV, and subtracting it from the 0 Cs^+ records to remove capacity transients and linear leak currents. (Series resistance, 8.5 MΩ; cell capacitance, 16 pF.)

RESULTS

The aim of these experiments is to quantify ionic selectivity of I_h channels. We first present the basic features of I_h and our approach to measuring reversal potentials.

Features of I_h

Fig. 1 *A* shows current recordings made in a 20 mM K^+ solution without and with 2 mM Cs^+ to block I_h. The traces on the right are difference currents, representing the Cs^+-sensitive component. The I_h channels are closed at the holding potential of −33 mV. A hyperpolarizing conditioning voltage step to −113 mV activates a slowly developing inward I_h current, and test steps to more positive voltages turn the

current off again. The reversal potential was determined from "instantaneous" current–voltage (*I-E*) relations (Fig. 1 *B*), which for the Cs^+-sensitive difference current (filled circles) is curved and crosses the voltage axis at −35 mV, defining the reversal potential. The curvature is an artifact of the Cs^+ subtraction procedure. The block of I_h channels by Cs^+ is much less complete at positive potentials than at negative potentials (DiFrancesco, 1982), and therefore the difference current at positive potentials reflects only a fraction of the I_h that is flowing. Nevertheless, this subtraction procedure does not affect the reversal potential for I_h. In the absence of Cs^+ the current is $I_{other}(E) + I_h(E)$, and the current in the presence of Cs^+ is $I_{other}(E) + [1\text{-}f(E)]I_h(E)$, where $f(E)$ is the fraction of I_h blocked by Cs^+ at voltage E. Therefore, the difference current is $f(E)I_h(E)$, which will have the reversal potential of I_h. This assumes that I_h is the only Cs^+-sensitive current and that Cs^+ ions themselves are not permeant (see Discussion).

Fig. 1 *B* illustrates that in 20 mM K^+ the instantaneous *I-E* relation derived by a conventional linear leak subtraction (open circles) is much more linear and gives the

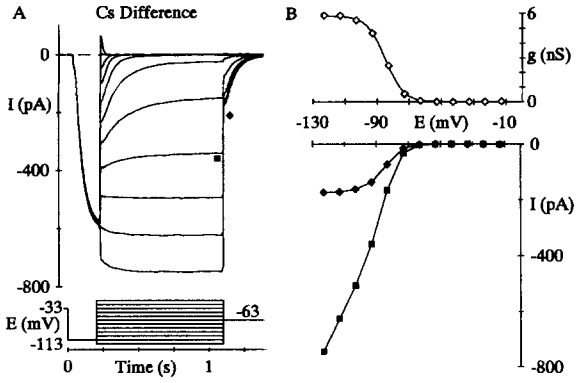

FIGURE 2. Activation of I_h. (*A*) Cs^+-difference current for a rod in 20 mM K^+ solution. The most negative test potential is −123 mV. (*B*) Steady-state (*filled squares*) and tail current amplitudes (*filled diamonds*) plotted against test potential. Steady-state activation curve (*open diamonds*), expressed in units of conductance, is derived from tail current amplitudes (see Materials and Methods). Smooth curve was fitted with the Boltzmann equation. (9.5 MΩ; 18.5 pF.)

same reversal potential as Cs^+ subtraction. However, as the contaminating I_{Kx} is voltage and time dependent and, in some solutions, larger than I_h, this method often will fail to isolate I_h on its own. The decaying tail of inward current most evident in the hyperpolarization steps in Figs. 4, 9, and 10 (in 2 mM Cs^+) is I_{Kx}.

Fig. 2 is an experiment to measure the voltage dependence of the activation of I_h channels using tail currents. The membrane potential is stepped to −113 mV, as before, to open I_h channels, and then returned to various potentials for 900 ms, both to measure the reversal potential and to allow I_h gating to relax to equilibrium (Fig. 2 *A*). This gives the steady-state currents plotted as squares in Fig. 2 *B*. Finally, the potential is stepped to −63 mV, where the fraction of open channels at each test potential can be measured by the amplitude of the tail current (solid diamonds). The steady-state currents show the inwardly rectifying nature of I_h gating, and the tails show that opening of the channels is steeply voltage dependent between −74 and −94 mV, with a maximal number of I_h channels being activated negative to −113

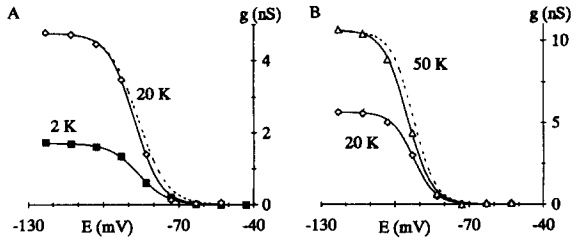

FIGURE 3. Changing external K^+ does not affect I_h gating. Steady-state activation curves, derived as in Fig. 2 *B*, for different external K^+ concentrations. (*A*) Rod in 2 K, 18 NMDG, or 20 K solution (tail potential, −73 mV). *Dashed line,* Boltzmann fit to 2 mM K^+ record, scaled by 2.79. (*B*) A different rod in 20 K, 30 NMDG, or 50 K solution (tail potential, −63 mV). *Dashed line,* Boltzmann fit to 20 mM K^+ record, scaled by 1.87.

mV. The tail currents are transformed into conductances (open diamonds) to yield an activation curve that is fitted by the following Boltzmann parameters (smooth line): g_{max}, 5.8 nS; $E_{1/2}$, −85.5 mV; and Q, 4.7. An activation curve derived from the 20 K, 0 Cs record was essentially identical: g_{max}, 5.9 nS; $E_{1/2}$, −85 mV; and Q, 4.6.

Activation curves measured from tail currents in the same way with 2, 20, and 50 mM K^+ are shown in Fig. 3. Increasing the K^+ concentration increases the maximum conductance of I_h channels appreciably but has little effect on the midpoint and steepness of the activation curve (summarized in Table I).

Ammonium (NH_4^+) Is Permeant

We turn now to identify permeant ions other than K^+. With some ions the Cs^+-difference currents are small and have a different time course from that of I_h in 20 mM K^+. In 20 mM NH_4^+, without Cs^+, there are time-dependent currents (mostly I_{Kx}) whose time course is not entirely similar to that of I_h (Fig. 4 *A*). However, Cs^+

TABLE I

Boltzmann Parameters for Steady-State Activation Curves Measured in Different K^+ Concentrations or Permeant Monovalent Cations

X	g_{max}	$E_{1/2}$	Q	n	E^*
	nS	*mV*			*mV*
2 K^+	1.9 ± 0.1	−93 ± 2	5.1 ± 0.3	3	−73
20 K^+	5.1 ± 0.3	−94 ± 2	5.5 ± 0.2	6	−73
5 K^+	2.7 ± 0.2	−98 ± 2	5.3 ± 0.4	4	−53
20 K^+	4.5 ± 0.2	−97 ± 1	5.3 ± 0.2	6	−53
50 K^+	8.8 ± 0.3	−94 ± 0.5	5.0 ± 0.2	3	−63
20 K^+	4.6 ± 0.4	−91 ± 2	5.7 ± 0.2	4	−63
20 NH_4^+	0.6 ± 0.05	−76.5 ± 0.5	4.3 ± 0.3	4	−54
20 K^+	4.9 ± 0.2	−84 ± 1	5.0 ± 0.3	4	−53
20 MA	1.1 ± 0.05	−79 ± 3	4.1 ± 0.1	3	−74
20 K^+	5.4 ± 0.5	−90 ± 2	4.5 ± 0.2	4	−73
20 Na^+	0.6	−88	4.7	2	−49
20 K^+	5.2 ± 0.3	−88 ± 3	4.8 ± 0.1	3	−48

Activation curves for 20 K^+ were measured in the same rod before and/or after that for the test solution.
*Tail test potential.

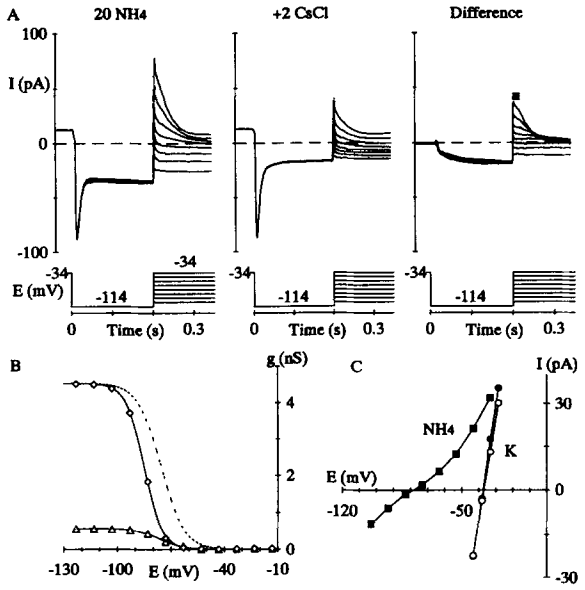

FIGURE 4. Permeation of NH_4^+. (*A*) A rod bathed in 20 mM NH_4^+ test solution. (*B*) Steady-state activation curves for a rod bathed in 20 K (*diamonds*) or 20 NH_4^+ (*triangles*) solution (tail potential, −53 mV). *Dashed line*, Boltzmann fit to NH_4^+ record scaled by 8.1. (*C*) Instantaneous *I-E* relation for the Cs^+-difference current and for the same rod in 20 K solution before (*filled circles*) and after (*open circles*) exposure to 20 NH_4^+ (*filled squares*). (7 MΩ; 19.5 pF.)

subtraction reveals currents that activate slowly at −114 mV and deactivate at more positive potentials, much like I_h currents in 20 mM K^+. The activation curve (Fig. 4 *B*) of these currents in NH_4^+, measured as in Fig. 2, shows a somewhat more positive midpoint (−76 instead of −85 mV), a lower slope (Q = 3.9 instead of 5.0), and a much lower maximal conductance (0.54 instead of 3.5 nS), as is summarized in Table I. The reversal potential for currents in NH_4^+ is almost 50 mV more negative than in K^+ (Fig. 4 *C*), showing that NH_4^+ is less permeable, and giving in seven cells a mean permeability ratio P_{NH_4}/P_K of 0.17 (Table II).

Several Larger Amines Are Not Measurably Permeant

When ethylammonium ($EtNH_3^+$) is the test cation, the Cs^+-difference current is small and *outward* at all test potentials down to −154 mV. Nevertheless, the time

TABLE II

ΔE_r and Permeability Ratios for Organic Cations

X	ΔE_r ± SEM	P_X/P_K	*n*
	mV		
K^+	0	1.0	
Ammonium	−44 ± 1.7	0.17	7
Methylammonium	−71 ± 2.0	0.06	9
Hydrazine (pH 5.75)	−81 ± 3.5	0.04	6
Dimethylammonium	> −100	< 0.02	8
Ethylammonium	> −120	< 0.01	4
Tetramethylammonium	> −120	< 0.01	9

Reference and test solution: 20 XCl, 90 TEACl, 18 glucose, 5 histidine, except for hydrazine, where the buffer was 10 MES titrated with TMAOH.

dependence of this outward current seems to correspond to gating of I_h channels. At −114 mV there is a slow increase of conductance and at −64 mV there is a slow decrease (Fig. 5 *A*). The reversal potential is shifted by at least −120 mV (Fig. 5 *B*), indicating that the permeability relative to K^+ must be <0.01 (Table II). When the K^+ solution is returned, the normal I_h returns undiminished and with the expected reversal potential (Fig. 5 *B*). Two other amines of similar or larger size than $EtNH_3^+$, dimethylammonium and tetramethylammonium (TMA), gave similar results

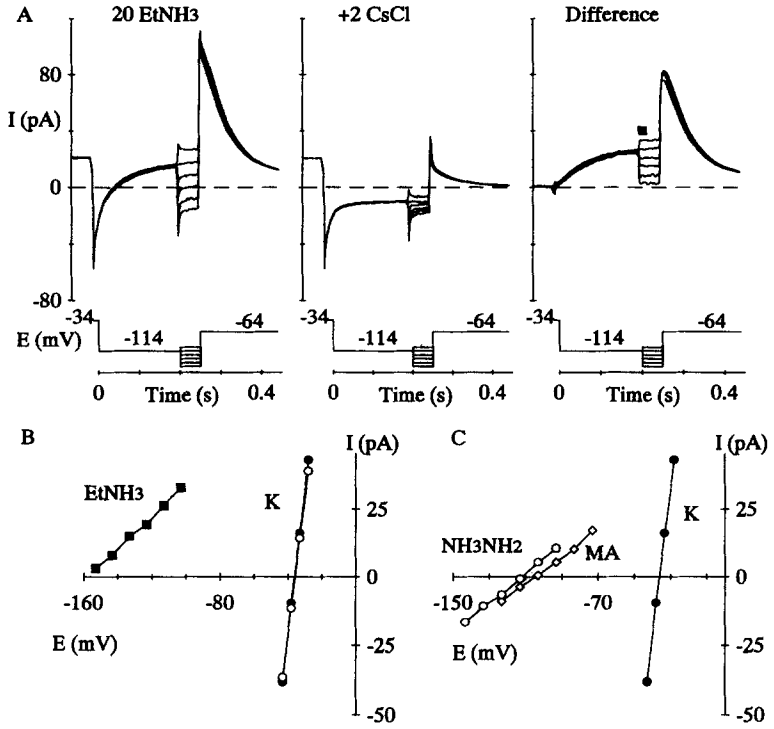

FIGURE 5. Ethylammonium is poorly permeant. (*A*) A rod bathed in $EtNH_3^+$ test solution. The most negative test potential was −153 mV. (*B*) Instantaneous *I-E* relation for the Cs^+-difference current and for the same rod in 20 K reference solution before (*filled circles*) and after (*open circles*) exposure to 20 $EtNH_3$ (*filled squares*). (*C*) Instantaneous *I-E* relation for Cs^+-difference currents for different rods tested in hydrazine ($NH_2NH_3^+$, *circles*) or methylammonium (MA, *diamonds*). (5.5 MΩ; 12.5 pF.)

(Table II). Two smaller amines, hydrazine and methylamine, had a small but measurable permeability, shifting the reversal potential by −81 and −71 mV (Table II). To be sure that the small inward currents in these cations were not due to an incomplete washout of K^+ ions from the control solution, we switched first to the TMA solution, in which only outward currents were obtained, before going to the hydrazine or methylammonium solutions (Fig. 5 *C*).

Na^+ and K^+ Ions Are Both Permeant

The reversal potential for I_h changes when the external K^+ concentration is changed (Fig. 6 *A*). In the absence of Na^+, the measured values agree well with the predictions of the Nernst equation for a K^+ electrode (Fig. 6 *B*), showing that I_h channels are much more permeable to K^+ ions than to any of the other cations in these internal and external solutions. The Na^+ ion is also known to be permeant (DiFrancesco, 1981*b*; Mayer and Westbrook, 1983; Bader and Bertrand, 1984), a result we confirm. When 30 mM Na^+ is added to the 20 mM K^+ solution (Fig. 7 *A*), the reversal potential shifts ~6 mV more positive (Fig. 7 *B*), consistent with a permeability ratio

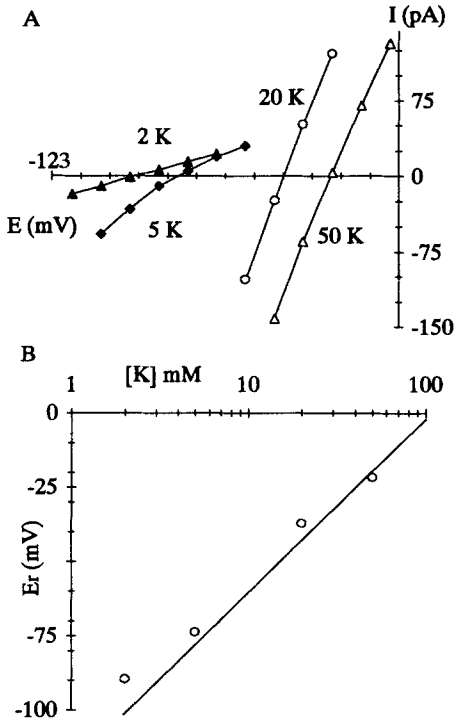

FIGURE 6. K^+ selectivity of I_h channels. (*A*) Instantaneous *I-E* relations for rods bathed in 2, 5, 20, or 50 mM K^+. NMDG was substituted for K^+ to maintain osmolarity. Records for 2 and 5 K are derived from Cs^+-difference currents, and for 20 and 50 K from ohmic leak subtraction. (*B*) Average reversal potentials (number of rods) for: 2 K, −90 ± 1.5 mV (n = 4); 5 K, −74 ± 1.0 mV (n = 4); 20 K, −37 ± 0.6 mV (n = 12); 50 K, −22 ± 0.5 mV (n = 3). Standard error bars are smaller than symbols. Straight line is derived from Nernst potential for K^+ electrode: E_K = (25.5 mV) ln $\{[K]_o/[K]_i\}$, where $[K]_i$ = 108 mM.

P_{Na}/P_K of 0.36 ± 0.02 (n = 3).

Whole-cell currents change substantially when K^+ ions are removed from Na^+-containing solutions. The Cs^+-difference current is inward at −114 mV, but surprisingly shows little time dependence there (Fig. 8 *A*). Subsequent test steps to more positive potentials turn off an outward current that looks like I_h. Although the currents are smaller, the shape of a steady-state activation curve measured in the usual way from tails is the same in 20 mM Na^+ as that for I_h in 20 mM K^+ solution (Fig. 8 *B*; Table I). The reversal potential of the instantaneous currents is shifted by −27 mV (Fig. 8 *C*) and the calculated mean permeability ratio P_{Na}/P_K is 0.33 (Table III), in good accord with the results in Na-K mixtures.

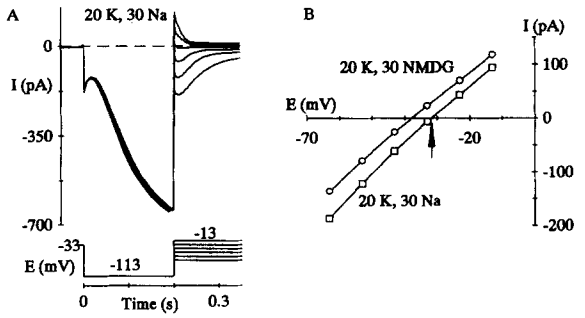

FIGURE 7. Permeability to Na^+. (*A*) A rod bathed in 20 mM K^+, 30 mM Na^+ solution. (*B*) Leak-subtracted instantaneous *I-E* relations for currents in *A* (*open squares*) and for the same rod with 30 mM NaCl replaced by 30 mM NMDG (*open circles*). Arrow indicates E_r calculated from the GHK voltage equation (see Materials and Methods), assuming that only K^+ and Na^+ are permeant, $P_{Na}/P_K = 0.36$ and $[Na]_i = 0$. (6 MΩ; 16.5 pF.)

Metal Ions: Tl^+ and Rb^+

We used KNO_3 as a reference solution in measuring the relative permeability of Tl^+; the reversal potentials for the Cs^+-difference current in KNO_3 and KCl were identical. Fig. 9 shows whole-cell currents for a rod bathed in a 20 mM $TlNO_3$, 90 mM $TEANO_3$ solution. In 0 Cs, whole-cell currents are large and comparable to those in the 20 mM KNO_3 reference solution and in 20 mM KCl. Further, with conditioning steps to −112 mV, there is a time-dependent inward current in the 0 Cs and the Cs^+-difference current. With test steps returning to more positive potentials, however, difference currents show essentially no time dependence, nor are they outward even at very positive potentials. One possible explanation is that Tl^+ reduces the block by Cs^+. However, in the 20 mM Tl^+, 0 Cs record, there are only small time-dependent currents at positive potentials, possibly reflecting only capacity transient currents. Also, in this example we used a fivefold higher concentration of

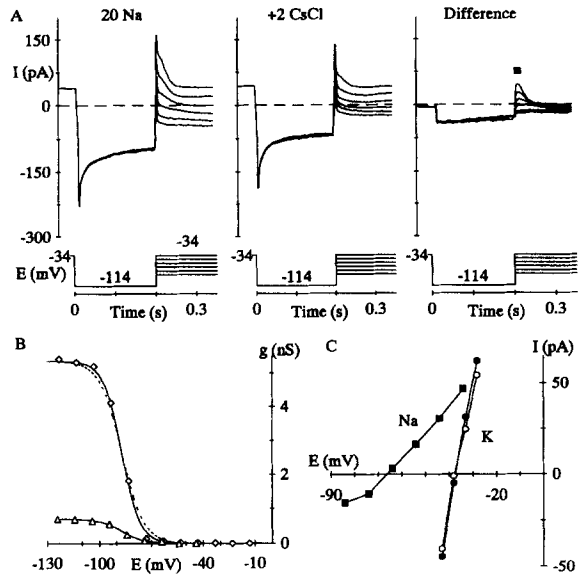

FIGURE 8. Reversal of I_h in 20 mM Na^+, 0 K^+. (*A*) A rod bathed in 20 mM Na^+ test solution. (*B*) Steady-state activation curves for a rod bathed in 20 K (*diamonds*) or 20 Na (*triangles*) solutions (tail potential −48 mV). *Dashed line*, Boltzmann fit to Na^+ record scaled by 7.6. (*C*) Instantaneous *I-E* relation for Cs^+-difference current in 20 mM K^+ solution before (*filled circles*) and after (*open circles*) exposure to 20 Na (*filled squares*). (9 MΩ; 21 pF.)

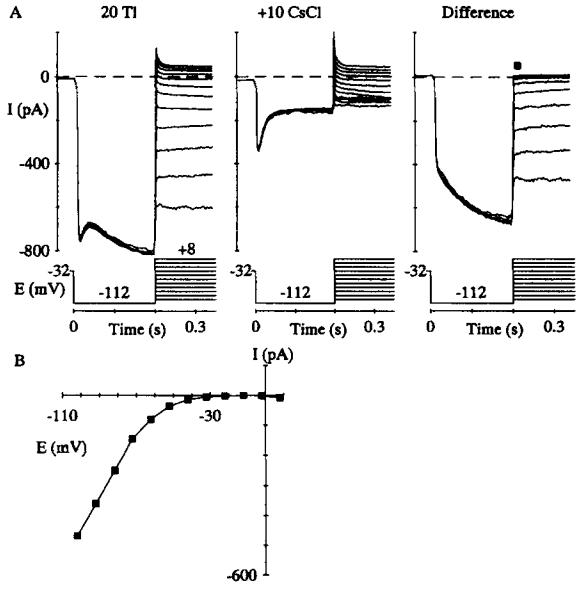

FIGURE 9. Permeability to Tl^+. (*A*) Rod bathed in 20 mM $TlNO_3$, 90 mM $TEANO_3$ with 0 (*left*) or 10 mM (*center*) added CsCl. The 10 mM Cs^+-difference record is shown at right. (*B*) Instantaneous *I-E* relation for 10 mM Cs^+-difference current (*filled squares*). (4 MΩ; 18.5 pF.)

Cs^+. Because of the lack of outward current, the Cs^+-sensitive instantaneous *I-E* relation in Tl^+ (closed squares) does not have a defined reversal potential (Fig. 9 *B*). In any case, clear *inward* currents are present at potentials negative to −30 mV and P_{Tl}/P_K can be estimated to be > 1.55 (Table III).

Like Cs^+, Rb^+ blocks I_h channels (DiFrancesco, 1982; Wollmuth, L. P., and B. Hille, unpublished data), but Cs^+ and Rb^+ seem to block at different sites and Rb^+ is much less efficacious. Fig. 10 *A* shows that when Rb^+ is the test cation there still is a large Cs^+-sensitive inward current. However, this current shows no time dependence either with the conditioning step or, like the Tl^+ difference current, with positive test steps. Despite the lack of time dependence, there are properties of this Cs^+-sensitive current that suggest that it flows through I_h channels. The steady-state currents in Rb^+ and K^+ appear at the same potentials (Fig. 10 *B*). In addition, the Cs^+-sensitive current in Rb^+ is completely blocked by 500 μM 9-amino-1,2,3,4-tetrahydroacridine (n = 3), a blocker of the time-dependent component in K^+ solutions (DiFrancesco,

TABLE III

ΔE_r and Permeability Ratios for Alkali Metal and Thallous Cations

X	ΔE_r ± SEM	P_X/P_K	n
	mV		
K^+	0	1.0	
Na^+	−28 ± 1.4	0.33	9
Li^+	−96 ± 2.3	0.02	7
Rb^+	< −16	> 0.55	7
Tl^+*	> +10	> 1.55	7

Reference and test solution: 20 XCl, 90 TEACl, 18 glucose, 5 histidine.
*Reference and test solution: 20 XNO_3, 90 $TEANO_3$, 18 glucose, 5 histidine.

Porciatti, Janigro, Maccaferri, Mangoni, Tritella, Chang, and Cohen, 1991; Wollmuth, L. P., and B. Hille, unpublished data), and it persists even in 2 mM $BaCl_2$ ($n = 2$), a blocker of most K^+ channels, and in 0.1 mM $CdCl_2$. Fig. 10 *C* shows the instantaneous *I-E* relation in Rb^+. Again, since there is no outward current the reversal potential is not defined, but it must be positive to −60 mV. Hence, P_{Rb}/P_K is > 0.55 (Table III).

Relative Conductance

Another measure of selectivity is relative conductance. In measuring relative conductance we used 0 Cs records, since the block of I_h channels by Cs^+ gets stronger at more negative potentials. Steady-state *I-E* plots (cf. Fig. 10 *B*), which were leak-subtracted by fitting a line to positive potentials, were fitted with a line over the very

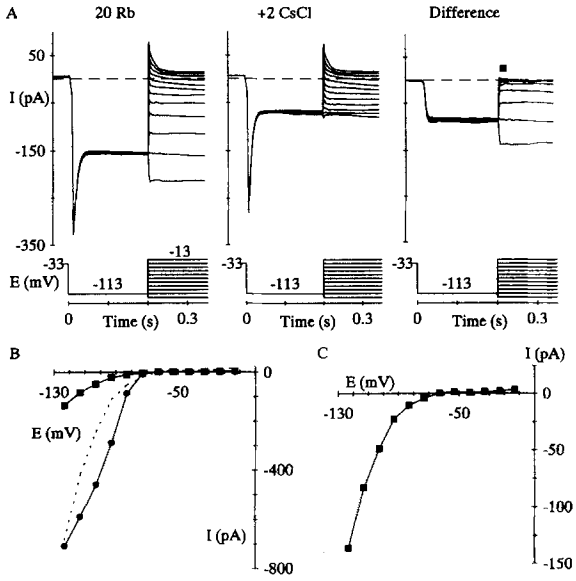

FIGURE 10. Possible Rb^+ permeability. (*A*) A rod bathed in 20 mM Rb^+ test solution. (*B*) Steady-state *I-E* relation for Cs^+-difference currents in 20 Rb (*squares*) or 20 K (*circles*). *Dashed line*, Rb record scaled by 5. (*C*) Instantaneous *I-E* relation for Cs^+-difference current. (9 MΩ; 21 pF.)

negative region to derive the steady-state limiting slope conductance (G). The conductance was normalized to 20 K. The relative conductance (G_X/G_K) was: Tl^+, 1.07; K^+, 1; Rb^+, 0.37; NH_4^+, 0.07; Na^+, 0.02. Each value has a minimum of three observations.

DISCUSSION

Identification of the Current

This paper describes measurements of Cs^+-sensitive currents in photoreceptors using solutions containing 90 mM TEA. An important and not completely resolved issue is whether the current sensitive to 2 mM Cs^+ is exclusively I_h or is contaminated by other currents. In K^+- or amine-containing solutions, the Cs^+-sensitive current has all the kinetic features of I_h, both with hyperpolarization and with subsequent depolar-

ization (Figs. 1, 4, and 5). However, with K^+-free Na^+, Tl^+, or Rb^+ solutions, not all of the expected kinetic features are seen; with Na^+ there is no I_h-like time dependence during the hyperpolarizing pulse (Fig. 8), with Tl^+ there is none during the depolarizing pulse (Fig. 9), and with Rb^+ there is none during either pulse (Fig. 10). Three hypotheses need be considered: (*1*) The Cs^+-sensitive currents seen are flowing in other channels. (*2*) The ionic conditions alter I_h channels so that they do not conduct in the outward direction and therefore gating cannot be observed. (*3*) Permeant ions have profound effects on the gating of I_h channels. Hypotheses *2* and *3* could be closely related.

Consider hypothesis *1*, that other channels are involved. Salamander rods have conventional voltage-gated Ca and K channels, I_{Kx} channels, and Ca^{2+}-activated Cl and K channels (Bader et al., 1982; Beech and Barnes, 1989). These are, however, not good candidates to carry a Cs^+-sensitive, inwardly rectifying Na^+, Tl^+, or Rb^+ current at potentials between −130 and −60 mV. As there may be still other channels, such as inward rectifiers, hypothesis *1* remains possible and difficult to exclude. One possibility is that the presence of Na^+, Rb^+, or Tl^+ interferes with the action of Cs^+ on I_h channels (so that I_h would no longer be isolated as the difference current). This would seem more likely if the difference currents in Na^+, Rb^+, or Tl^+ could not be blocked by other blocking agents of I_h channels. However, we find here that, like the normal difference currents in K^+ (DiFrancesco et al., 1991; our results), the unusual currents in Rb^+ are blocked by 500 μM 9-amino-1,2,3,4-tetrahydroacridine but not by 2 mM Ba^{2+}, a blocker of many K channels including inward rectifiers (Rudy, 1988).

Hypothesis *2* might be applied to Tl^+ or Rb^+ solutions, where no outward currents are seen. It would suggest that complete replacement of K^+ with Tl^+ or Rb^+ greatly reduces the ability of the I_h channel to carry outward currents. Indeed, some such postulate seems necessary since we know that I_h channels are present in the membrane and that permeant K^+ ions are present inside the cell, yet no outward current is observed. Remotely analogous examples in the literature are the establishment of normal inward rectification in cardiac i_{K1} (and other) channels by internal Mg^{2+} (Vandenberg, 1987; Matsuda, Saigusa, and Irisawa, 1987) and the absolute requirement of certain K channels for extracellular K^+ ions to conduct outward current at all (Carmeliet, 1989; Pardo, Heinemann, Terlau, Ludewig, Lorra, Pongs, and Stühmer, 1992). Such properties presumably depend on occupancy of ion-binding sites at or within the pore and indeed we find that I_h channels have numerous flux properties suggestive of multiple binding sites in the pore (Wollmuth and Hille, 1992).

An alternative but similar explanation for the apparently instantaneous nature of rectification in, for example, Rb^+ is that normal I_h channel gating has become very fast (hypothesis *3*) at all voltages. This would fit well with the finding that the voltage dependence of the steady-state K^+ and Rb^+ conductances are nearly superimposable (Fig. 10 *B*) and that the currents in Rb^+ are sensitive to the aminoacridine blocker. The literature does give several examples of major changes of channel gating occurring when an ion is added or taken away from the medium. For example, the skeletal muscle inward rectifier is a time-dependent increasing current in K^+ but a time-dependent decreasing current in Tl^+ (Stanfield, Ashcroft, and Plant, 1981;

Ashcroft and Stanfield, 1983). Also, in the delayed rectifier of squid giant axons, activation gating is slowed by intracellular fluoride (Adams and Oxford, 1983) and by extracellular Zn^{2+} (Gilly and Armstrong, 1982), and closing is lost when extracellular Ca^{2+} is removed (Armstrong and Lopez-Barneo, 1987; Armstrong and Miller, 1990).

Perhaps the most difficult records to identify with I_h channels are the difference currents in Na^+ (Fig. 8). Here all currents are small and even a small contamination would be significant. With steps to −114 mV the difference current is only −30 pA and shows little time dependence. Nevertheless, the tails during steps back to more positive potentials do show a time course like the deactivation of I_h. In addition, they have three other properties expected of I_h currents: Activation curves constructed with these tails indicate that they depend on preceding hyperpolarizing pulses with exactly the same voltage dependence as currents in K^+ (Fig. 8 *B*). Furthermore, the tails grow with increasing duration of the activation pulse much as they do in K^+ solution (Wollmuth and Hille, 1992). Finally, the reversal potential measured from the tails gives the same P_{Na}/P_K as that from larger I_h currents in Na^+/K^+ mixtures. Therefore we suggest that I_h channels are activating normally in Na^+ solution during the hyperpolarizing prepulse; however, as no time dependence is seen in the small inward current measured at −114 mV, this may be contaminated with current in some other channel. Apparently in K^+-free Na^+ solutions, the ability of the channels to conduct inward current is highly attenuated. In cardiac cells, the ability of the I_h-like current I_f to carry inward Na^+ currents also depends on external K^+ (Frace, Maruoka, and Noma, 1992).

Selectivity of I_h Channels

Others have shown that I_h is carried by both K^+ and Na^+ (DiFrancesco, 1981*b*; Mayer and Westbrook, 1983; Bader and Bertrand, 1984; Hestrin, 1987). When P_{Na}/P_K has been explicitly calculated, it was for mixtures of Na^+ and K^+ as in Fig. 7 giving values from 0.2 to 0.3 (Hestrin, 1987; Maricq and Korenbrot, 1990). In mixtures of external K^+ and Na^+, we found P_{Na}/P_K to be 0.36, and with only Na^+ outside and K^+ inside it was 0.33.

Edman and Grampp (1989) addressed the permeability of ions other than K^+ and Na^+ in I_h channels. They tested Li^+, hydrazine, NH_4^+, and Rb^+ and concluded that none permeated I_h channels. However, permeabilities were tested in the presence of K^+ and calculated from the change in amplitude of the time-dependent current recorded at a constant voltage. A major drawback of this approach is that it assumes independence of permeant ions. This condition is not met in I_h channels, which are blocked by some permeant ions (NH_4^+, Tl^+, Rb^+; Wollmuth and Hille, 1992), have permeability ratios that depend on permeant ion concentrations (Hestrin, 1987), and show anomalous mole fraction dependence (Wollmuth and Hille, 1992). Measurements of changes in reversal potentials are insensitive to these deviations from independence (Hille, 1971).

Comparison to Other Channels

I_h channels have been called nonselective cation channels since they are permeable to Na^+ and K^+. Yet, in comparison to other "nonselective" cation channels such as the nicotinic acetylcholine receptor (nAChR) channel or the cGMP-gated channel in rod

outer segments, this one is highly selective. The nAChR channel, for example, is almost equally permeable to all alkali metal ions and is permeated by >41 organic cations and several divalent cations (Dwyer et al., 1980; Adams et al., 1980). Further, ethylammonium, which is essentially impermeant in I_h channels, has a permeability equal to that of K^+ in nAChR channels.

The selectivity of I_h channels shows few similarities to that of Na channels. In Na channels, Li^+ and hydroxylamine are about equally permeant, whereas hydrazine is half as permeant as Na^+ (Hille, 1971, 1972). We were unable to assess the permeability of hydroxylamine since rods became unstable in the presence of this ion, but I_h channels show a very low permeability to Li^+ ($P_{Li}/P_{Na} = 0.06$) and hydrazine ($P_{hydrazine}/P_{Na} = 0.12$). Perhaps more revealing, in Na channels P_K/P_{Na} is <0.1, whereas in I_h channels it is almost 3.

The selectivities of I_h and K channels show few similarities and a significant difference. Like K channels (Hille, 1973), I_h channels are permeable to Tl^+, Rb^+, and NH_4^+. Nevertheless, they differ in that I_h channels have a relatively high permeability to Na^+. For most K channels, the P_{Na}/P_K is <0.03.

Possible Explanations for Selectivity

Our results with organic cations allow us to estimate the diameter of the most restricted part of the pore. Ammonium ions are reasonably permeant ($P_{NH_4}/P_K = 0.17$) and have a diameter of 3.7 Å, assuming that all hydrogens can form hydrogen bonds. Methylammonium (MA) is also permeant ($P_{MA}/P_K = 0.06$). It is a linear molecule with a methyl group at one end and an amine group at the other. The methyl group, which cannot form hydrogen bonds, has a diameter of 4 Å, so the minimum profile diameter for MA is dictated by the methyl group. In contrast, ethyl- and dimethylammonium are essentially impermeant. They are slightly larger than MA with a minimum profile diameter of ~4.6 Å. Hence, the minimum pore diameter of I_h channels seems to be between 4 and 4.6 Å (based on Corey-Pauling space-filling models). These dimensions are larger than those for K and Na channels but smaller than those for nAChR channels (Dwyer et al., 1980).

I_h channels display properties that seem to put them in a class of their own within the superfamily of voltage-gated channels: like Na, Ca, and delayed rectifier K channels, I_h channels have steeply voltage-dependent gating and activate with a sigmoid time course, but unlike the others they also deactivate with a sigmoid time course. Like inward rectifier channels, I_h channels open at negative potentials, close at positive potentials, and are blocked by Cs^+ and Rb^+ ions. Unlike inward rectifier channels, however, they have a high permeability to Na^+, have a nearly linear instantaneous *I-E* relation, are not strongly blocked by Ba^{2+} ions, and have a voltage dependence that does not shift with changes of external K^+.

We thank M. Shapiro, K. P. Mackie, Y. B. Park, and A. Tse for their comments on the manuscript, Lea Miller for secretarial assistance, and Don Anderson for technical assistance.

This work was supported by a National Institutes of Health research grant, NS-08174, a Research Award from the McKnight Endowment for the Neurosciences (B. Hille), and an NIH training grant, GM-07108 (L. P. Wollmuth).

Original version received 27 February 1992 and accepted version received 17 August 1992.

REFERENCES

Adams, D. J., T. M. Dwyer, and B. Hille. 1980. The permeability of endplate channels to monovalent and divalent metal cations. *Journal of General Physiology.* 75:493–510.

Adams, D. J., and G. S. Oxford. 1983. Interaction of internal anions with potassium channels of the squid giant axon. *Journal of General Physiology.* 82:429–448.

Armstrong, C. M., and J. Lopez-Barneo. 1987. External calcium ions are required for potassium channel gating in squid axons. *Science.* 236:712–714.

Armstrong, C. M., and C. Miller. 1990. Do voltage-dependent K^+ channels require Ca^{2+}? A critical test employing a heterologous expression system. *Proceedings of the National Academy of Sciences, USA.* 87:7579–7582.

Ashcroft, F. M., and P. R. Stanfield. 1983. The influence of the permeant ions thallous and potassium on inward rectification in frog skeletal muscle. *Journal of Physiology.* 343:407–428.

Attwell, D., F. S. Werblin, and M. Wilson. 1982. The properties of single cones isolated from the tiger salamander retina. *Journal of Physiology.* 328:259–283.

Attwell, D., and M. Wilson. 1980. Behaviour of the rod network in the tiger salamander retina mediated by membrane properties of individual rods. *Journal of Physiology.* 309:287–315.

Bader, C. R., D. Bertrand, and E. A. Schwartz. 1982. Voltage-activated and calcium-activated currents studied in solitary rod inner segments from the salamander retina. *Journal of Physiology.* 331:253–284.

Bader, C. R., and D. Bertrand. 1984. Effect of changes in intra- and extracellular sodium on the inward (anomalous) rectification in salamander photoreceptors. *Journal of Physiology.* 347:611–631.

Bader, C. R., P. R. Macleish, and E. A. Schwartz. 1979. A voltage-clamp study of the light response in solitary rods of the tiger salamander. *Journal of Physiology.* 296:1–26.

Barnes, S., and B. Hille. 1989. Ionic channels of the inner segment of tiger salamander cone photoreceptors. *Journal of General Physiology.* 94:719–743.

Beech, D. J., and S. Barnes. 1989. Characterization of a voltage-gated K^+ channel that accelerates the rod response to dim light. *Neuron.* 3:573–581.

Carmeliet, E. 1989. K^+ channels in cardiac cells: mechanisms of activation, inactivation, rectification and K_e^+ sensitivity. *Pflügers Archiv.* 414:S88–S92.

DiFrancesco, D. 1981*a*. A new interpretation of the pace-maker current in calf Purkinje fibres. *Journal of Physiology.* 314:359–376.

DiFrancesco, D. 1981*b*. A study of the ionic nature of the pace-maker current in calf Purkinje fibres. *Journal of Physiology.* 314:377–393.

DiFrancesco, D. 1982. Block and activation of the pacemaker channel in calf Purkinje fibres: effects of potassium, caesium, and rubidium. *Journal of Physiology.* 329:485–507.

DiFrancesco, D., F. Porciatti, D. Janigro, G. Maccaferri, M. Mangoni, T. Tritella, F. Chang, and I. S. Cohen. 1991. Block of the cardiac pacemaker current (I_f) in the rabbit sino-atrial node and in canine Purkinje fibres by 9-amino-1,2,3,4-tetrahydroacridine. *Pflügers Archiv.* 417:611–615.

Dwyer, T. M., D. J. Adams, and B. Hille. 1980. The permeability of the endplate channel to organic cations in frog muscle. *Journal of General Physiology.* 75:469–492.

Edman, A., and W. Grampp. 1989. Ion permeation through hyperpolarization-activated membrane channels (*Q*-channels) in the lobster stretch receptor neurone. *Pflügers Archiv.* 413:249–255.

Frace, A. M., F. Maruoka, and A. Noma. 1992. External K^+ increases Na^+ conductance of the hyperpolarization-activated current in rabbit cardiac pacemaker cells. *Pflügers Archiv.* 421:94–96.

Gilly, W. F., and C. M. Armstrong. 1982. Divalent cations and the activation kinetics of potassium channels in squid giant axons. *Journal of General Physiology.* 79:965–996.

Goldman, D. E. 1943. Potential, impedance, and rectification in membranes. *Journal of General Physiology.* 27:37–60.

Hamill, O. P., A. Marty, E. Neher, B. Sakmann, and F. J. Sigworth. 1981. Improved patch-clamp techniques for high-resolution current recording from cells and cell-free membrane patches. *Plügers Archiv.* 391:85–100.

Hestrin, S. 1987. The properties and function of inward rectification in rod photoreceptors of the tiger salamander. *Journal of Physiology.* 390:319–333.

Hille, B. 1971. The permeability of the sodium channel to organic cations in myelinated nerve. *Journal of General Physiology.* 58:599–619.

Hille, B. 1972. The permeability of the sodium channel to metal cations in myelinated nerve. *Journal of General Physiology.* 59:637–658.

Hille, B. 1973. Potassium channels in myelinated nerve: selective permeability to small cations. *Journal of General Physiology.* 61:669–686.

Hodgkin, A. L., and A. F. Huxley. 1952. A quantitative description of membrane current and its application to conduction and excitation in nerve. *Journal of Physiology.* 117:500–544.

Hodgkin, A. L., and B. Katz. 1949. The effect of sodium ions on the electrical activity of the giant axon of the squid. *Journal of Physiology.* 108:37–77.

Maricq, A. V., and J. I. Korenbrot. 1990. Inward rectification in the inner segment of single retinal cone photoreceptors. *Journal of Neurophysiology.* 64:1917–1928.

Matsuda, H., A. Saigusa, and H. Irisawa. 1987. Ohmic conductance through the inwardly rectifying K channel and blocking by internal Mg^{2+}. *Nature.* 325:156–159.

Mayer, M. L., and G. L. Westbrook. 1983. A voltage-clamp analysis of inward (anomalous) rectification in mouse spinal sensory ganglion neurones. *Journal of Physiology.* 340:19–45.

Pardo, L. A., S. H. Heinemann, H. Terlau, U. Ludewig, C. Lorra, O. Pongs, and W. Stühmer. 1992. Extracellular K^+ specifically modulates a rat brain K^+ channel. *Proceedings of the National Academy of Sciences, USA.* 89:2466–2470.

Rudy, B. 1988. Diversity and ubiquity of K channels. *Neuroscience.* 25:729–749.

Spain, W. J., P. C. Schwindt, and W. E. Crill. 1987. Anomalous rectification in neurons from cat sensorimotor cortex in vitro. *Journal of Neurophysiology.* 57:1555–1576.

Stanfield, P. R., F. M. Ashcroft, and T. D. Plant. 1981. Gating of a muscle K^+ channel and its dependence on the permeating ion species. *Nature.* 289:509–511.

Vandenberg, C. A. 1987. Inward rectification of a potassium channel in cardiac ventricular cells depends on internal magnesium ions. *Proceedings of the National Academy of Sciences, USA.* 84:2560–2564.

Wollmuth, L. P., and B. Hille. 1991. Permeability and block in I_h channels of rod photoreceptors. *Biophysical Journal.* 59:269*a*. (Abstr.)

Wollmuth, L. P., and B. Hille. 1992. Mechanism of ion permeation in I_h channels. *Biophysical Journal.* 61:289*a*. (Abstr.)

Yanagihara, K., and H. Irisawa. 1980. Inward current activated during hyperpolarization in the rabbit sinoatrial node. *Pflügers Archiv.* 385:11–19.